Supporting Information

Iodide-mediated intermediate regulation strategy enables high-capacity and ultra-stable zinc-iodine batteries

Zhijie Xu[a], Jiaqi Yang[a], Peng Sun[b], Yaoyu Chen[a], Zhengxiao Ji[a], Xusheng Wang[c], Min Xu*[a], Jinliang Li*[b], Likun Pan*[a]

[a] Shanghai Key Laboratory of Magnetic Resonance, School of Physics and Electronic Science, Institute of Magnetic Resonance and Molecular Imaging in Medicine, East China Normal University, Shanghai 200241, China.

[b] Siyuan Laboratory, Guangdong Provincial Engineering Technology Research Center of Vacuum Coating Technologies and New Energy Materials, College of Physics & Optoelectronic Engineering, Department of Physics, Jinan University, Guangzhou 510632, China.

[c] State Key Laboratory of Bio-based Fiber Materials, School of Materials Science and Engineering, Zhejiang Sci-Tech University, Hangzhou 310018, P. R. China.

Experimental

Materials

All experimental reagents used were of analytical grade and were not further purified. Zinc sulfate heptahydrate ($ZnSO_4 \cdot 7H_2O$, AR, 99.5%) and ultrahigh capacitance porous activated carbon (PAC, specific surface area: 1800 m^2 g^{-1}, granularity: 5-8 μm) were purchased from Shanghai Aladdin Biochemical Technology Co., Ltd. Iodine (I_2, 99.8%) and zinc iodide (ZnI_2, AR, 98%) were purchased from Shanghai Macklin Biochemical Co., Ltd. Sodium carboxymethyl cellulose (CMC) and styrene butadiene rubber emulsion (SBR) were purchased from Guangdong Canrd New Energy Technology Co., Ltd. Glass fiber separator (Whatman GF/C) with a thickness of 260 μm was purchased from Sigma-Aldrich. Both 0.1 mm thick zinc foil and 0.02mm thick titanium foil were purchased from Wenghou Metal Materials Business Firm, Shushan District, Hefei City.

Preparation of I_2@PAC cathode

The I_2@PAC material was prepared via the solution adsorption method. Briefly, 1.2 g I_2 and 1 g PAC were added into 200 mL deionized water, followed by continuous stirring for 3 days. Then vacuum filtration, drying at 60℃ for 12h to remove excess iodine to obtain I_2@PAC. The iodine ratio in the I_2@PAC composite was 53.4 wt%, as proved by the TG test. The I_2@PAC, CMC, SBR and super P were mixed in deionized water with a mass ratio of 8:0.5:0.5:1. Then the slurry was cast on a titanium foil followed by drying for 12 h in the air at 60 °C. The electrodes were cut into disks with a diameter of 14 mm.

Preparation of the electrolytes

ZSO electrolyte was prepared by dissolving 57.51 g $ZnSO_4 \cdot 7H_2O$ in 100 mL deionized water. By adding 0.01 M, 0.02 M, 0.05 M, 0.1 M, and 0.2 M zinc iodide (ZnI_2) to ZSO, the electrolytes ZSO-0.01, ZSO-0.02, ZSO-0.05, ZSO-0.1, and ZSO-0.2 were obtained.

Material characterizations

The thermogravimetric analysis of I_2@PAC materials were performed on a HITACHI STA200 simultaneous thermal analyzer with a heating rate of 10 °C/min from room temperature to 800 ℃ at N_2 atmosphere. The morphologies of Zn deposits on the Zn-metal anodes and EDS tests were detected by

SEM (HITACHI S-4800). The I_2@PAC materials and Zn deposits were conducted by XRD (Holland Panalytical PRO PW3040/60, Cu Kα λ=1.54056 Å). In situ Raman spectra (WeTec alpha300R) testing system consisting of Raman spectrometer (532 nm laser) with per-Raman spectrum in voltage internal of 0.1 V, electrochemical workstation (CV test at 0.5 mV s^{-1}), a computer, and an Operando Raman cell (Tianjin Aida Hengsheng Sci. & Tech. Co. Ltd., China) was utilized with I_2@PAC, separator, and zinc foil with a hole in the middle. All the Operando Raman spectra information collected was raw, untreated data. The electrical conductivity of the electrolytes was tested using a DDSJ-308F conductivity meter (Instruments and Electronics Shanghai Associates). Meanwhile, the pH value of the electrolytes was measured with a PHS-25 pH meter (Instruments and Electronics Shanghai Associates).

Electrochemical measurements

The electrochemical performances of Zn||Zn cells, Zn||Ti cells, Zn||Cu cells, and Zn||I_2@PAC cells were assembled using electrode discs as the working electrodes, Zn foil (100 μm) as the counter electrode, and glass fiber (Whatman GF/C) as the separator, with 120 μL of electrolyte, and the cells were assembled using a pressure of 50 kg cm^{-2}. Galvanostatic cycling tests were conducted on a Land2001A battery test system in the voltage range of 0.6-1.6 V (vs. Zn^{2+}/Zn). The specific capacities of the Zn||I_2@PAC cells were calculated based on the mass of the cathode iodine. Impedance measurements were performed using (CHI-660E) within a frequency range of 1 MHz to 0.01 Hz. The CV measurements were performed from 0.6 to 1.6 V on autolab (PGST A302N) electrochemical workstation at scan rates varying from 0.1 to 1 mV s^{-1}. The LSV measurements were conducted on autolab electrochemical workstation at a scan rate of 1 mV s^{-1}. The GITT test, consisting of a series of current pulses (0.2 A g^{-1}) for 2 min followed by a 8 min relaxation process, was performed with the voltage range from 0.6 V to 1.6 V (vs. Zn^{2+}/Zn). The Tafel curves were tested with an overpotential from -150 mV to 150 mV (vs. Zn^{2+}/Zn).

DRT analysis

DRT deconvolution used the EIS impedance data, and it was used to unravel various processes in the Zn-I_2 cells.

DRT impedance, $Z_{\mathrm{DRT}}(f)$, at a frequency f, can be expressed as:[1]

$$Z_{DRT}(f) = i2\pi f L_0 + R_\infty + \int_{-\infty}^{+\infty} \frac{\gamma(\log \tau)}{1 + i2\pi f \tau} d\log \tau \#(1)$$

where L_0, R_∞, τ, and $\gamma(\log \tau)$ are an inductance, an ohmic resistance, a timescale, and the DRT, respectively. In turn, the total polarization resistance, R_{pol}, was computed using the following integral:

$$R_{pol} = \int_{-\infty}^{+\infty} \gamma(\log \tau) d\log \tau \#(2)$$

Process the data using Prof. Ciucci's DRTtools, with parameter settings referenced from their work.[2]

RTC calculations

The intensity ratio R of (hkl) plane was calculated by the following equation:

$$R(hkl) = \frac{I(hkl)}{\sum I(h_i k_i l_i)} \#(3)$$

where I(hkl) is the intensity of the (hkl) plane in XRD profile, and $\sum I(h_i k_i l_i)$ is the sum of intensity of all crystal planes in XRD profile. Texture coefficient (TC) and relative texture coefficient (RTC) were calculated using the following formula:[3]

$$TC(hkl) = \frac{R_1(hkl)}{R_2(hkl)} \#(4)$$

$$RTC(hkl) = \frac{TC(hkl)}{\sum TC(h_i k_i l_i)} \#(5)$$

where $R_1(hkl)$ and $R_2(hkl)$ represent the calculated ratio by Equation (3) of the sample and reference sample (standard Zn, PDF#04-0831), respectively.

Calculation of Ion Diffusion Coefficient (D):

The Zn^{2+} ion diffusion coefficient (D) in the active material can be calculated by following equation:[4]

$$D = \frac{4}{\pi\tau}\left(\frac{m_B V_m}{M_B S}\right)^2 \left(\frac{\Delta E_S}{\Delta E_\tau}\right)^2 \#(6)$$

where τ is the duration of the current pulse; m_B refers to the mass of the active material on the cathode; V_m is the molar volume of the active material; M_B refers to the molar mass of the active material; S is the electrode-electrolyte interface area; ΔE_S refers to the voltage change between two adjacent equilibrium states; and ΔE_τ is the voltage change induced by the galvanostatic charge/discharge. The detailed parameters in ZSO and ZSO-0.1 electrolytes can be found in Table S6.

DFT calculations

The first-principal calculations were conducted utilizing spin-polarized density functional theory (DFT) within the CASTEP module.[5] The electron exchange correlation was described by the gradient-corrected Perdew-Burke-Ernzerh (GGA-PBE) functional.[6] Ion-electron interaction was described by the projector augmented-wave (PAW) method.[7] The cutoff energy was established at 480 eV, with the total energy and force convergence for geometric optimization set at 10^{-5} eV and 0.02 eV/Å, respectively. For structural relaxation, a grid of 3 × 3 × 1 Gamma-centered k-points was employed, DFT-D3 was used for van der Waals correction. The formation energy (E_{form}) was defined by the following formula:

$$E_{form} = E_{C+I_5^-} - E_{C+I_2} - E_{C+I_3^-} \#(7)$$

With this definition, a more negative formation energy indicates I_5^- ion on the C surface is thermodynamically favorable. Based on established literature, we adopted the linear I_3^- and V-shaped I_5^- configurations for modeling.[8, 9]

Computational methods of MD

All the MD simulations were performed using the GROMACS 2020.6 software package.[10] Low density simulation boxes containing randomly distributed Zn^{2+}, SO_4^{2-}, I^- were created by Packmol.[11] The initial volume for each box was taken to be 10 × 10 × 10 nm^3. Details of all systems are listed in Table S1. H_2O module was modeled using 3-site SPC/E parameters. Van der Waals and bonded parameters (bonds, angles, improper dihedrals, and torsions) were based on the GROMOS 54A7 force field.[12] Before the simulations, the structures were optimized using the steepest descent minimization method until the system energy was reduced to below 10.0 kJ/mol. NVT equilibrations were performed at 298.15 K for 0.1 ns, followed by NPT equilibration at 298.15 K and 1.0 atm for 0.1 ns. The resulting configurations were then used for further equilibration runs.

The production runs were performed for 10 ns with the pressure maintained at 1.0 atm and the temperature at 298.15 K. During both equilibration and production runs, the temperature was controlled using V-rescale coupling method[13] (coupling time of 0.1 ps) and the pressure was controlled using the Parrinello-Rahman coupling method (coupling time of 2.0 ps). Periodic boundary conditions were implemented. Visual Molecular Dynamics (VMD) tools were used to observe the MD simulation results and analyze radial distribution functions (RDF) and coordination number (CN) between different

groups.[14]

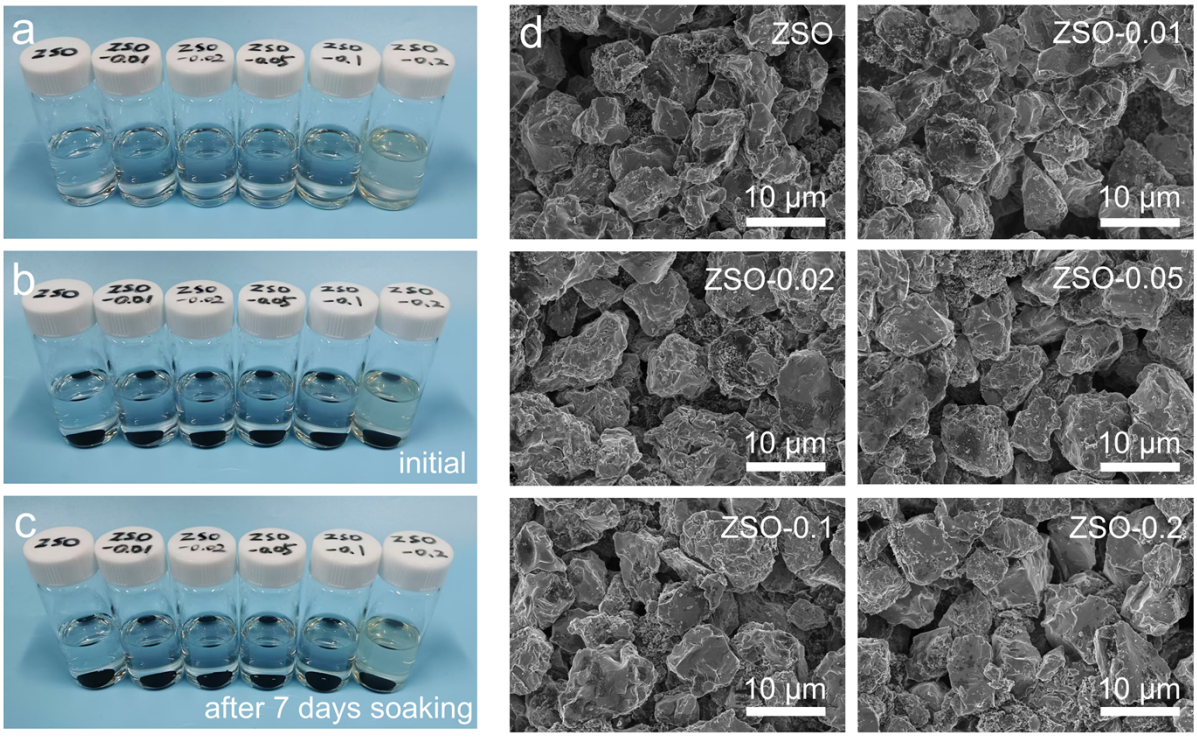

Figure S1. (a) Optical photographs of prepared ZSO, ZSO-0.01, ZSO-0.02, ZSO-0.05, ZSO-0.1 and ZSO-0.2. (b) Initial state after I_2@PAC cathode soaking and (c) after 7 days soaking. (d) SEM images of I_2@PAC cathode after 7 days soaking.

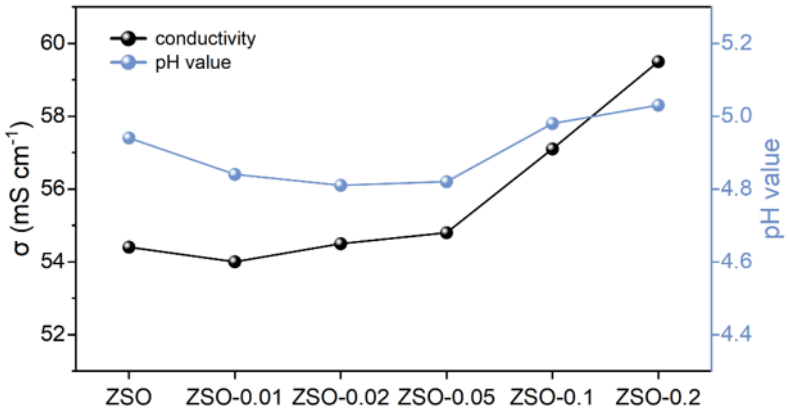

Figure S2. Ionic conductivity and pH value of electrolytes with different concentrations of iodide ions additives.

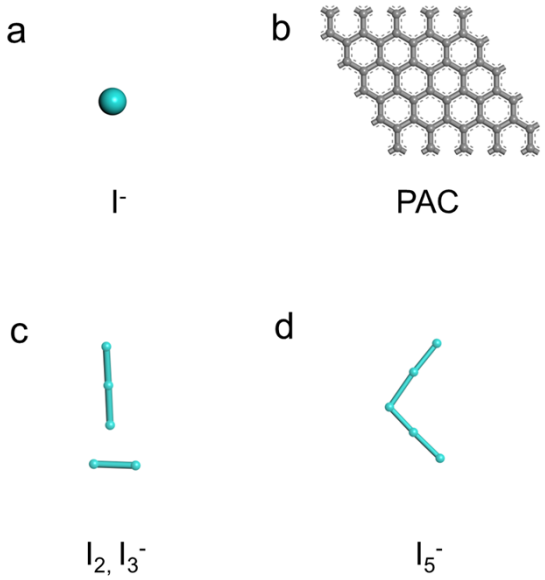

Figure S3. DFT models of I^-, PAC, I_2, I_3^- and I_5^- in vacuum.

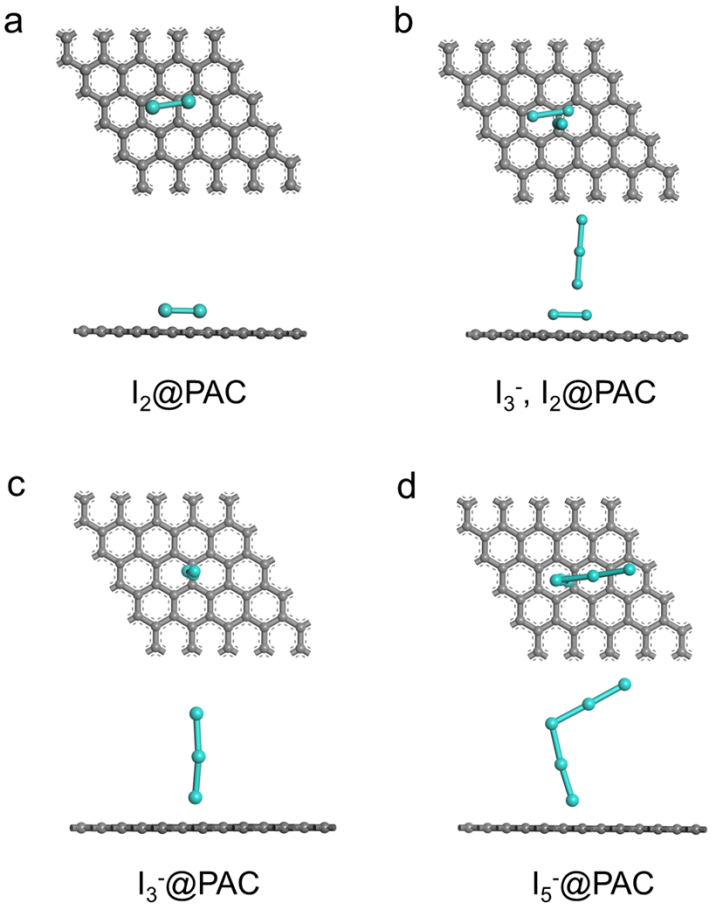

Figure S4. DFT models of I_2@PAC, I_3^-, I_2@PAC, I_3^-@PAC and I_5^-@PAC.

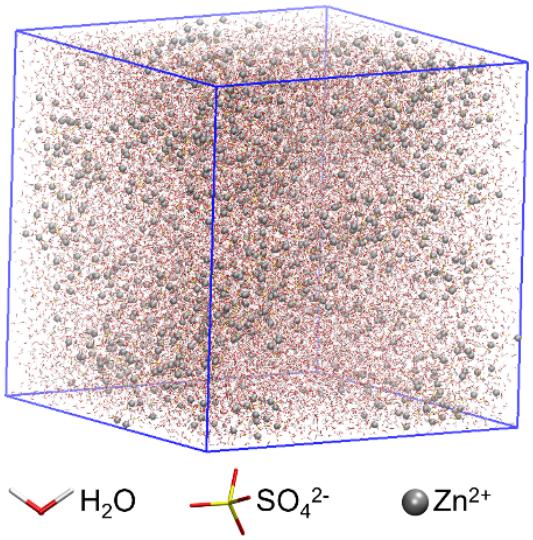

Figure S5. 3D snapshots of MD simulation for the ZSO-0.1 electrolyte.

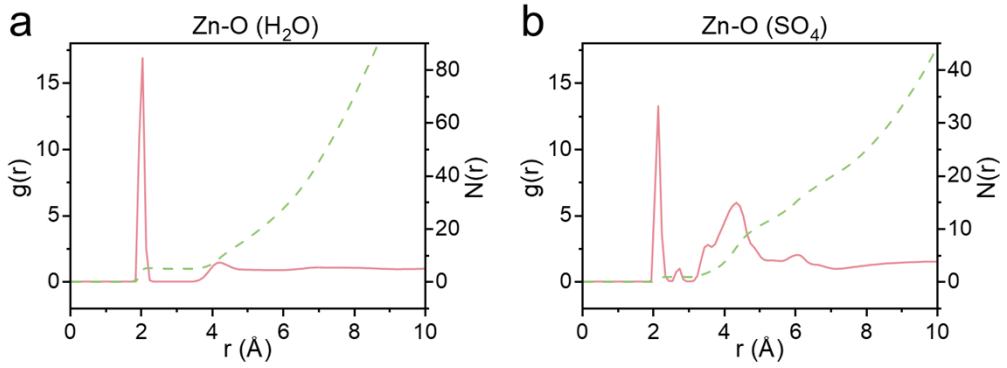

Figure S6. RDFs and the coordination number of (a) Zn-O (H_2O) and (b) Zn-O (SO_4) in ZSO electrolyte.

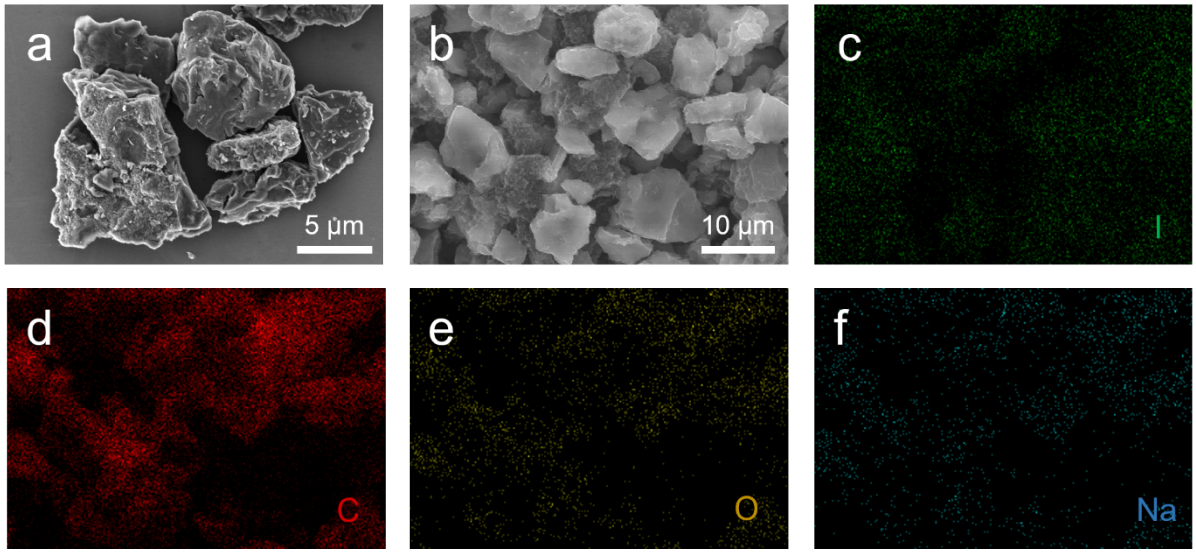

Figure S7. (a, b) SEM images and (c-e) EDS mapping of I_2@PAC cathode.

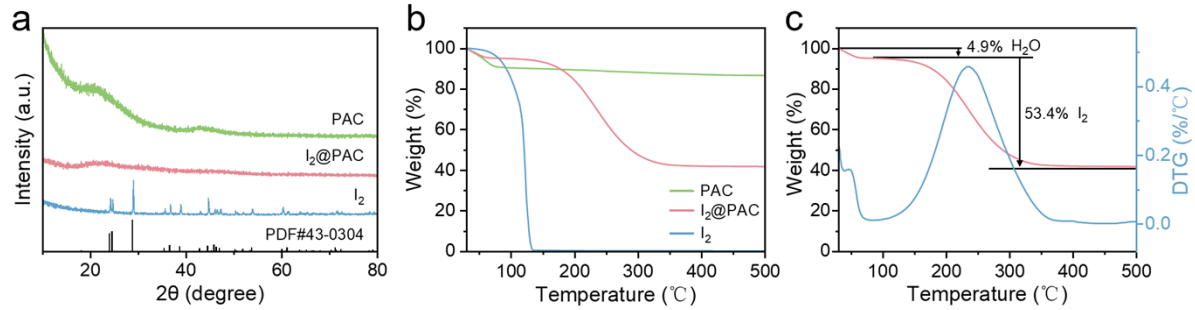

Figure S8. (a) XRD patterns of PAC, I_2@PAC, I_2, and PDF#43-0304 (standard I_2). (b) TG curves of PAC, I_2@PAC, I_2. (c) TG and DTG curves of I_2@PAC.

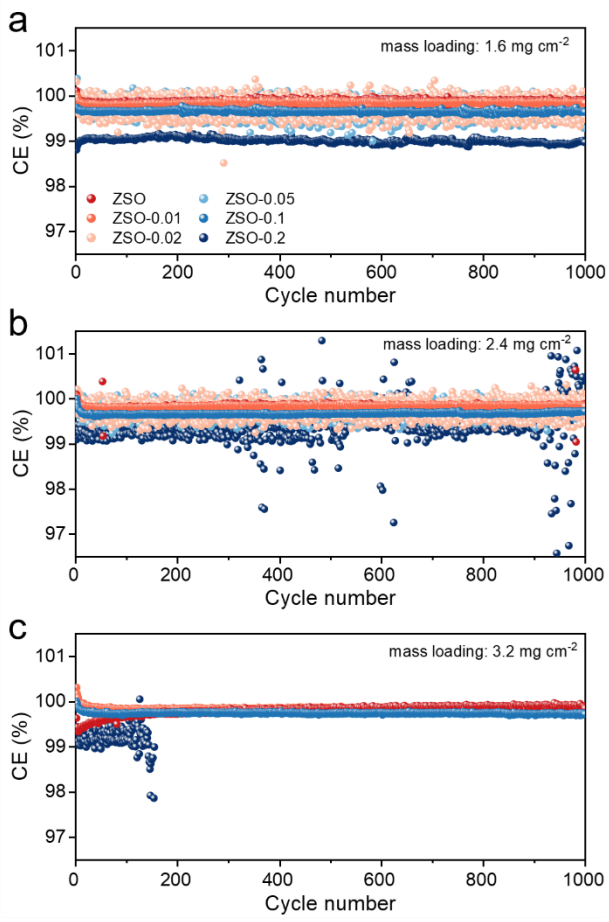

Figure S9. Coulomb efficiency of Zn||I_2@PAC full cells with different iodine mass loadings on the cathode: (a) 1.6 mg cm^{-2}, (b) 2.4 mg cm^{-2}, and (c) 3.2mg cm^{-2}.

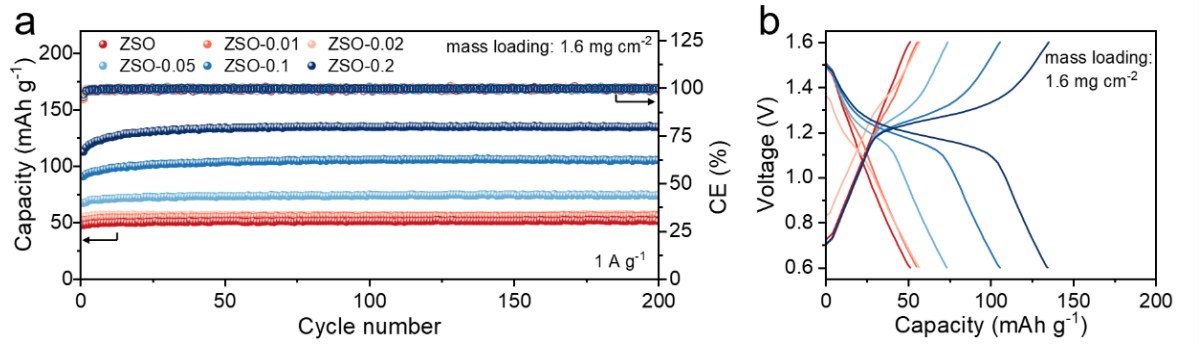

Figure S10. (a) Cycling performance of Zn||pure carbon cells in ZSO-x at 1 A g^{-1}. (b) Charge/discharge profiles of the 100th cycle for Zn||pure carbon cells in ZSO-x at 1 A g^{-1}.

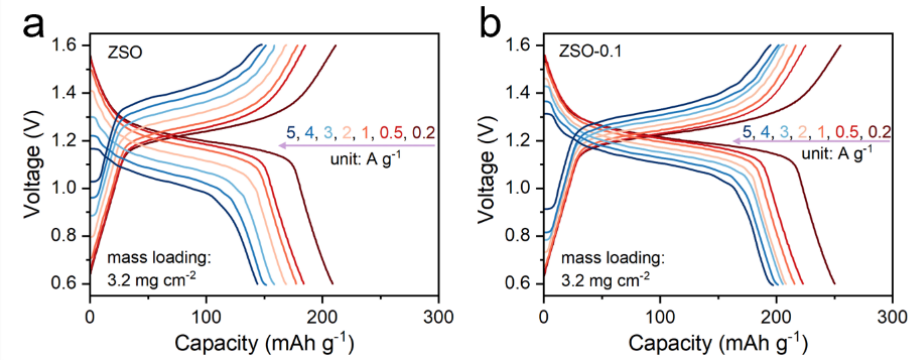

Figure S11. GCD curves of rate performance in (a) ZSO and (b) ZSO-0.1 with a mass loading of 3.2 mg cm^{-2}.

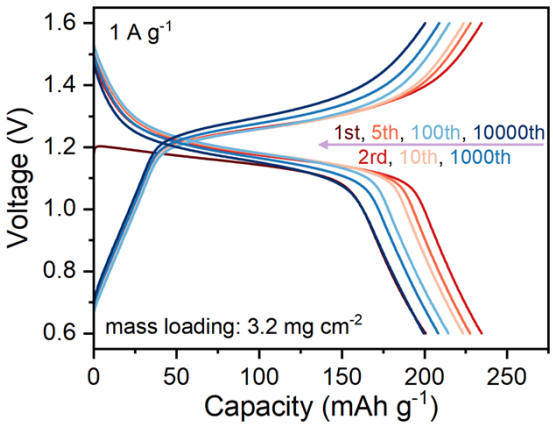

Figure S12. GCD profiles of specific cycle numbers during long-term cycling stability tests.

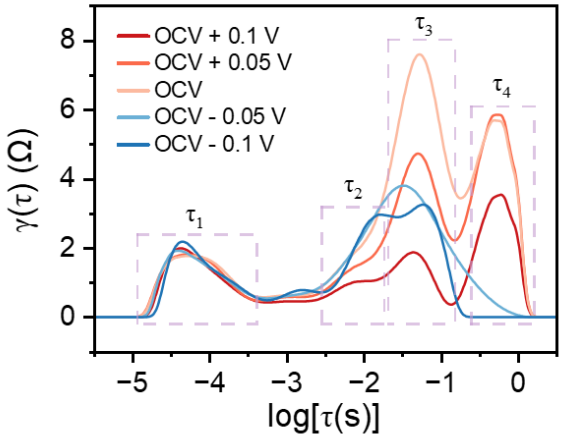

Figure S13. DRT profiles of the I_2@PAC electrode in ZSO-0.1 at OCV, OCV ± 0.05 V and OCV ± 0.1 V.

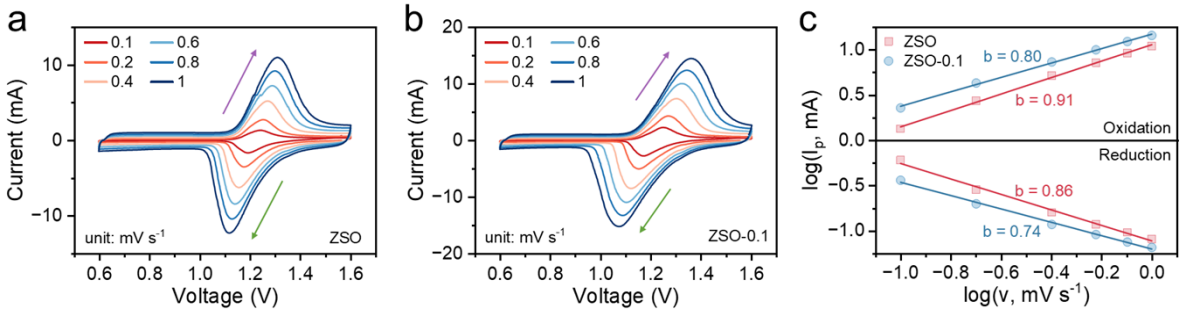

Figure S14. CV curves at different scan rates in (a) ZSO and (b) ZSO-0.1. (c) Plots of I_p vs. v at cathodic/anodic peak (I_p: peak current, v: scanning rate).

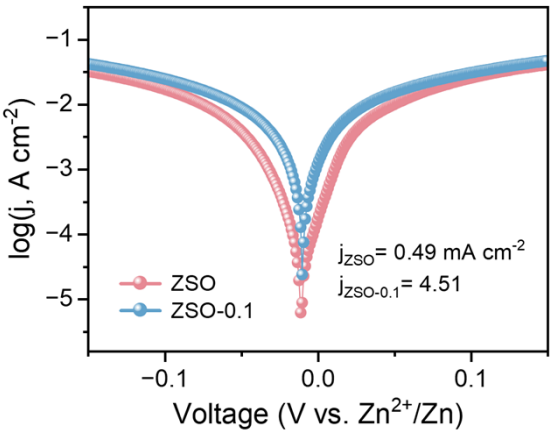

Figure S15. Tafel curves of Zn||Zn symmetric cells in ZSO and ZSO-0.1.

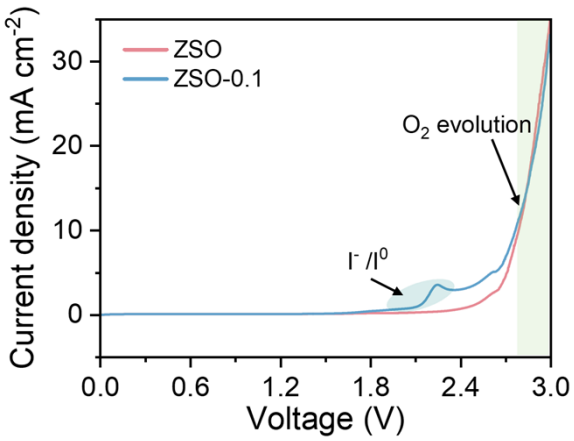

Figure S16. LSV curves of ZSO and ZSO-0.1 at a scan rate of 1 mV s^{-1}.

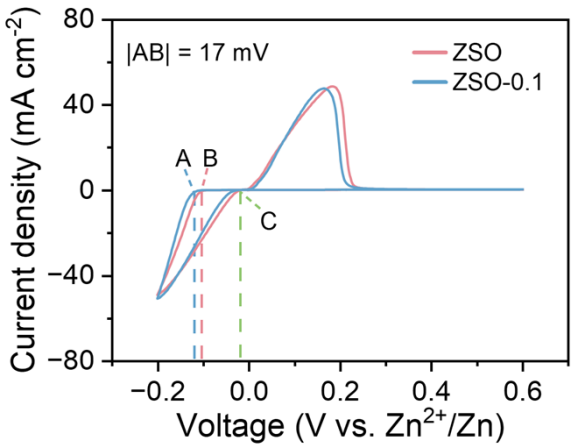

Figure S17. CV curves of Zn||Ti asymmetric cells in ZSO and ZSO-0.1 at a scan rate of 1 mV s^{-1} with a potential range of -0.2 V to 0.6 V.

Table S1 Element mass content from EDS results

Electrolyte	C	I	O	Zn	S
ZSO	47.13	42.53	6.38	2.80	0.92
ZSO-0.01	43.73	43.85	7.27	3.99	1.15
ZSO-0.02	44.74	46.99	4.81	2.43	0.45
ZSO-0.05	43.34	41.63	8.39	4.48	1.68
ZSO-0.1	44.49	40.38	8.25	4.59	1.68
ZSO-0.2	44.92	43.11	6.91	4.08	0.99

Table S2 Number of molecules in the MD simulations

System	Size	Number of molecules			
		Zn^{2+}	SO_4^{2-}	I^-	H_2O
ZSO-0.1	$10 \times 10 \times 10$ nm^3	1260	1200	120	30000
ZSO	$10 \times 10 \times 10$ nm^3	1200	1200	/	30000

Table S3 Comparison of main parameters and cycling performance for this work with prior studies

Electrolyte	Cathode	Capacity ($mAh\ g^{-1}/A\ g^{-1}$)	Capacity rention ($mAh\ g^{-1}$ / % / cycles)	Reference
2 M $ZnSO_4$ + 0.1 M ZnI_2	I_2@PAC	250.2 / 0.2	198 / 85 / 10000	This work
2 M $ZnSO_4$ + 0.1 M BMIS	I_2@KB	205 / 0.1	182.1 / 91.6 / 15000	[15]
1 M $Zn(Ac)_2$ + PVA (2.5 wt%)	PC/I_2 mixture	240 / 0.2	160 / 86 / 2600	[16]
2 M $ZnSO_4$ +0.2 M EMIM[OAc]	I_2@AC	223.6 / 0.4	149.2 / 76 / 18000	[17]
Catholyte: 0.1 M I_2 + 1 M LiI Anolyte: 12.5 M pyridine + 2 M $ZnSO_4$	Super P	180 /0.2	128 / 92 / 10000	[18]
Catholyte: 0.1 M I_2 + 1 M LiI Anolyte: 2 M $ZnSO_4$ + 15 mM Zn-PCA	Ketjen black	211 / 1	162 / 87 / 30000	[19]
Catholyte: 0.1 M I_2 + 1 M LiI Anolyte: 0.5 M $ZnSO_4$ + 0.5 M Li_2SO_4	Starch	180.5 / 0.2	70 / 90.5 / 50000	[20]
Zinc tetrafluoroborate hydrate and succinonitrile with molar ratio of 1:2	AC/I_2 mixture	202 / 0.5	125 / 75 / 10000	[21]
2 M $ZnSO_4$	I_2@iPOP-TPyPZn	178 / 0.5	153 / 80.5 / 40000	[22]
2 M $ZnSO_4$	I_2@Se_{SA}-NC-900	216 / 0.2	184 / 92 / 10000	[23]
2 M $ZnSO_4$	CFP/HEO-I_2	220 / 0.5	117 / 78.5 / 50000	[24]
2 M $ZnSO_4$	FeCoNi@I_2	139 / 0.2	108.8 / 79.5 / 13000	[25]

Table S4 Resistance value of ZSO electrolyte calculated from DRT curves

SoC (%)	R_1	R_2	R_3	R_4
0	1.87478	/	5.45377	3.10155
17	2.01613	/	1.5175	0.81347
33	2.07321	/	1.50476	0.7643
50	2.04864	/	1.23838	0.62629
67	2.04796	/	1.20322	0.62765
83	2.08257	/	1.44343	0.57084
100	2.12239	/	1.72745	0.54403
83	2.11945	/	2.45526	1.81654
67	2.09328	/	2.41903	1.48786
50	2.05796	/	2.45064	1.64431
33	2.18512	/	3.10865	2.0269
17	2.23052	/	4.10446	2.67201
0	2.24766	/	6.35273	4.75213

Table S5 Resistance value of ZSO-0.1 electrolyte calculated from DRT curves

SoC (%)	R_1	R_2	R_3	R_4
0	1.82029	1.55909	3.08079	2.31074
14	1.94955	1.59999	1.78592	1.36701
29	1.95379	1.40857	2.20977	1.38411
43	2.05294	1.56891	1.74063	1.19677
57	2.11636	1.90185	1.8322	1.46817
71	2.21625	2.18133	1.70151	1.64253
86	2.37609	3.09221	1.29151	1.27734
100	2.56587	4.59747	2.13293	2.27626
86	1.83308	1.77893	2.67452	2.38267
71	1.81326	1.21461	1.72059	1.66211
57	1.82982	0.89654	1.6227	1.46714
43	1.85661	1.01393	4.48429	6.01754
29	1.86141	1.07268	5.29254	7.68777
14	1.93364	1.04679	3.36105	3.43533
0	1.77995	1.2069	2.48081	2.45718

Table S6 Parameters for calculating the diffusion coefficient of Zn^{2+} in the cathode material

electrolyte	τ (s)	m_B (g)	M_B (g mol^{-1})	V_m (cm^3 mol^{-1})	S (cm^2)
ZSO	120	0.00392	126.9	25.74	1.54
ZSO-0.1	120	0.00556	126.9	25.74	1.54

References

1. J. R. Macdonald and M. K. Brachman, *Rev. Mod. Phys.*, 1956, **28**, 393-422.
2. J. Chen, E. Quattrocchi, F. Ciucci and Y. Chen, *Chem*, 2023, **9**, 2267-2281.
3. L. P. Bérubé and G. L'Espérance, *J. Electrochem. Soc.*, 1989, **136**, 2314.
4. Y. Zou, T. Liu, Q. Du, Y. Li, H. Yi, X. Zhou, Z. Li, L. Gao, L. Zhang and X. Liang, *Nat. Commun.*, 2021, **12**, 170.
5. D. Zhao, Z. Li, X. Yu, W. Zhou, Q. Wu, Y. Luo, N. Wang, A. Liu, L. Li and S. Chen, *Chem. Eng. J.*, 2022, **450**, 138254.
6. J. P. Perdew, K. Burke and M. Ernzerhof, *Phys. Rev. Lett.*, 1996, **77**, 3865-3868.
7. P. E. Blöchl, *Phys. Rev. B*, 1994, **50**, 17953-17979.
8. Y. Wang, Y. Xue, X. Wang, Z. Cui and L. Wang, *J. Mol. Struct.*, 2014, **1074**, 231-239.
9. M. Otsuka, H. Mori, H. Kikuchi and K. Takano, *Comput. Theor. Chem.*, 2011, **973**, 69-75.
10. M. J. Abraham, T. Murtola, R. Schulz, S. Páll, J. C. Smith, B. Hess and E. Lindahl, *SoftwareX*, 2015, **1-2**, 19-25.
11. L. Martínez, R. Andrade, E. G. Birgin and J. M. Martínez, *J. Comput. Chem.*, 2009, **30**, 2157-2164.
12. N. Schmid, A. P. Eichenberger, A. Choutko, S. Riniker, M. Winger, A. E. Mark and W. F. van Gunsteren, *Eur. Biophys. J.*, 2011, **40**, 843-856.
13. G. Bussi, D. Donadio and M. Parrinello, *J. Chem. Phys.*, 2007, **126**, 014101.
14. W. Humphrey, A. Dalke and K. Schulten, *J. Mol. Graph.*, 1996, **14**, 33-38.
15. H. Wu, J. Hao, S. Zhang, Y. Jiang, Y. Zhu, J. Liu, K. Davey and S.-Z. Qiao, *J. Am. Chem. Soc.*, 2024, **146**, 16601-16608.
16. Q. Yue, Y. Wan, X. Li, Q. Zhao, T. Gao, G. Deng, B. Li and D. Xiao, *Chem. Sci.*, 2024, **15**, 5711-5722.
17. T. Xiao, J.-L. Yang, B. Zhang, J. Wu, J. Li, W. Mai and H. J. Fan, *Angew. Chem. Int. Ed.*, 2024, **63**, e202318470.
18. Y. Lyu, J. A. Yuwono, P. Wang, Y. Wang, F. Yang, S. Liu, S. Zhang, B. Wang, K. Davey, J. Mao and Z. Guo, *Angew. Chem. Int. Ed.*, 2023, **62**, e202303011.
19. F. Wang, W. Liang, X. Liu, T. Yin, Z. Chen, Z. Yan, F. Li, W. Liu, J. Lu, C. Yang and Q.-H. Yang, *Adv. Energy Mater.*, 2024, **14**, 2400110.
20. S.-J. Zhang, J. Hao, H. Li, P.-F. Zhang, Z.-W. Yin, Y.-Y. Li, B. Zhang, Z. Lin and S.-Z. Qiao, *Adv. Mater.*, 2022, **34**, 2201716.
21. H. Xu, R. Zhang, D. Luo, J. Wang, K. Huang, J. Chi, H. Dou, X. Zhang and G. Sun, *Energy Storage Mater.*, 2023, **63**, 103019.
22. Y. Zhao, Y. Wang, W. Xue, H. Huang, J. Li, C. Hu and D. Liu, *Adv. Funct. Mater.*, 2025, 2422677.
23. Q. Liu, S. Wang, J. Lang, J. Wang, J. Zhan, H. Liu, Y. Qi, Z. Wu, H. Li, X. Lin and H. Li, *Nano Lett.*, 2025, **25**, 6661-6669.
24. Y. Li, H. Jia, Y. Hao, U. Ali, B. Liu, L. Zhang, L. Li, R. Lian and C. Wang, *Adv. Funct. Mater.*, 2025, **35**, 2419821.
25. Y. Gao, Y. Liu, X. Guo, J. Zhang, C. Zhou, F. Li, Z. Xu, Z. Zhao, Z. Xing, P. Rao, Z. Kang, X. Tian and X. Shi, *Adv. Funct. Mater.*, 2025, **35**, 2421714.